

Emerging Anisotropic Compact Stars in $f(\mathcal{G}, T)$ Gravity

M. Farasat Shamir ^{*} and Mushtaq Ahmad [†]

National University of Computer and Emerging Sciences,
Lahore Campus, Pakistan.

Abstract

The possible emergence of compact stars has been investigated in the recently introduced modified Gauss-Bonnet $f(\mathcal{G}, T)$ gravity, where \mathcal{G} is the Gauss-Bonnet term and T is the trace of the energy-momentum tensor [1]. Specifically, for this modified $f(\mathcal{G}, T)$ theory, the analytic solutions of Krori and Barua have been applied to anisotropic matter distribution. To determine the unknown constants appearing in Krori and Barua metric, the well-known three models of the compact stars namely 4U1820-30, Her X-I, and SAX J 1808.4-3658 have been used. The analysis of the physical behavior of the compact stars has been presented and the physical features like energy density and pressure, energy conditions, static equilibrium, stability, measure of anisotropy, and regularity of the compact stars, have been discussed.

Keywords: $f(\mathcal{G}, T)$ Gravity; Krori and Barua; Compact Stars.

PACS: 04.50.Kd; 04.20.Jb.

1 Introduction

In astrophysics, compact stars are generally being referred to as the white dwarfs, neutron stars including the hybrid and quark stars, and the black

^{*}farasat.shamir@nu.edu.pk

[†]mushtaq.sial@nu.edu.pk

holes. White dwarfs and neutron stars originated due to the degeneracy pressure produced by the fundamental particles responsible for their formation. These stars are massive but volumetrically smaller objects, therefore with high densities. Usually, the exact nature of these compact stars is not known to us but they are believed to be the massive objects with a small radius. Excluding black holes, all the other types of compact stars are sometimes also known as the degenerate stars. In general relativity (GR), an analysis of configured equilibrium is essential due to the reason of compact stars having huge mass and density. This can be started in a general relativistic way by considering the Oppenheimer-Volkoff equations [2] for static spherically symmetric and hydrostatic equilibrium, given as

$$\frac{dp}{dr} = -G \frac{(mc^2 + 4p\pi r^3)(\rho c^2 + p)}{r^2 c^4 - 2Gmc^2 r} \quad \text{and} \quad \frac{dm}{dr} = 4\rho\pi r^2, \quad (1)$$

where p , ρ , and m is the pressure, density, and mass of the star respectively, varying with radial coordinate r . At $r = R$ (the coordinate radius of the compact star), the total mass of compact star is determined as

$$M(R) = \int_0^R 4\pi r^2 \rho dr. \quad (2)$$

The combination of these Oppenheimer-Volkoff equations with the equation of the state (EoS) parameter $\omega = \frac{p}{\rho}$ when solved numerically results into different configurations of the compact stars with divisions of low and high densities [3, 4].

Schwarzschild [5] was the pioneer to present the spherically symmetric exact solutions of Einstein field equations. The outcome of the first solution was the exploration of space-time singularity which gave the idea of a black hole. The second non-trivial solution predicted the bounded compactness parameter i.e., $\mu(R) = \frac{2M(R)}{R} < \frac{8}{9}$ in hydrostatic equilibrium for some static and spherically symmetric configured structure [6]. Investigation of compact stars (neutron stars, dark stars, quarks, gravastars, and black holes) has become now an interesting research pursuit in astrophysics despite being not the new one. Baade and Zwicky [7] studied the compact stellar objects and argued that supernova may turn into a smaller dense compact object which came true later on after the discovery of pulsars which are highly magnetized rotating neutrons [8, 9]. Ruderman [10] was the first one to explore that at the core of the compact stars, the nuclear density turns anisotropic. A

number of investigations have been made to find the solutions of the field equations for spherically symmetric anisotropic configurations in different contexts [11]-[13]. The pressure of the fluid sphere splits into the tangential and radial pressures in anisotropic configurations. Different investigations reveal that the repulsive forces which construct the compact stars, are produced due to anisotropy. Kalam et al. [14] showed that the Krori and Barua metric [15] establishes the necessary conditions for the advocacy of an effective and stable approach in modelling the compact objects. From an integrated Tolman Oppenheimer-Volkoff (TOV) equation, the numerical simulations may be used to study the nature of the compact stars, using EoS parameter. Rahaman et al. [16, 17] used EoS Chaplygin gas to explore their physical characteristics by extending Krori and Barua models. Mak and Harko [18] used some standard models for spherically symmetric compact objects and explored exact solutions to find the physical parameters such as the energy density, radial and tangential pressures concluding that inside these stars, the parameters would remain positive and finite. Hossein et al. [19] studied the effects on anisotropic stars due to cosmological constant. Different physical properties such as mass, radius, and moment of inertia of neutron stars has been investigated and a comprehensive comparison has been established with GR and modified theories of gravity [20]. Some interesting investigations related to the structure of slow rotating neutron stars in R^2 gravity are accomplished by making use of two distinct hadronic and a strange matter EOS parameter [21]. For a comprehensive study, some fascinating results can be seen in [22]-[28].

As an alternative to the theory of GR, modified theories of gravity have played an important and pivotal role to reveal the hidden facts about the accelerating expansion of the universe. After being motivated by the original theory and using the complex lagrangian, modified theories of gravity like $f(R)$, $f(R, T)$, $f(\mathcal{G})$, and $f(R, \mathcal{G})$ have been structured, where R is the Ricci scalar, \mathcal{G} is the Gauss-Bonnet invariant term, and T is the trace of energy momentum tensor. Some reviews and important discussions relating to different modified theories of gravity have been published by different researchers [29]-[42]. Das et al. [43] presented exact conformal solutions to describe the interior of a star in modified teleparallel gravity. In another work, Das et al. [44] explored several physical features of the model admitting conformal motion to describe the behavior of the compact stars using modified $f(R, T)$ gravity. Sharif and Yousuf [45] investigated the stability conditions of collapsing object by considering the non-static and spherically

symmetric space-time. The field equations of $f(R, T)$ modified theory have been explored by implementing the perturbation approach [46]. The possible formation of compact stars in modified theory of gravity by using the Krori and Barua metric for spherically symmetric anisotropic compact stars has been discussed [47, 48]. In a recently published paper [1], Sharif and Ikram presented a new modified $f(\mathcal{G}, T)$ theory of gravity and studied different energy conditions for Friedmann-Robertson-Walker (FRW) universe. They found that the massive test particles follow non-geodesic geometry lines due to the presence of an extra force. It is being expected that the theory may describe the late-time cosmic acceleration for some special choices of $f(\mathcal{G}, T)$ gravity models. We discussed the Noether symmetry approach to find the exact solutions of the field equations in $f(\mathcal{G}, T)$ theory of gravity [49]. In another paper [50], we investigated the same modified Gauss-Bonnet $f(\mathcal{G}, T)$ gravity and used the Noether symmetry methodology to discuss some cosmologically important $f(\mathcal{G}, T)$ gravity models with anisotropic background reported for locally rotationally symmetric Bianchi type I universe. We used two models to explore the exact solutions and found that the specific models of modified Gauss-Bonnet gravity may be used to reconstruct Λ CDM cosmology without involving any cosmological constant. Thus it seems interesting to further explore the universe in this theory.

This paper is aimed to investigate the possible emergence of compact stars by constructing some viable stellar solutions in $f(\mathcal{G}, T)$ theory of gravity by choosing some specific models. The plan of our present study is as follows: In section 2, we give the fundamental formalism of $f(\mathcal{G}, T)$ gravity with anisotropic matter distribution. Section 3 is dedicated for the matching of the metric conditions. Some physical features of the present study in context of $f(\mathcal{G}, T)$ gravity model under consideration are given in Section 4. Lastly, we present some conclusive discussions.

2 Anisotropic Matter Distribution in $f(\mathcal{G}, T)$ Gravity

The general action for the modified $f(\mathcal{G}, T)$ is [1],

$$\mathcal{A} = \frac{1}{2\kappa^2} \int d^4x \sqrt{-g} [R + f(\mathcal{G}, T)] + \int d^4x \sqrt{-g} \mathcal{L}_M, \quad (3)$$

where the function $f(\mathcal{G}, T)$ consists of the Gauss-Bonnet term \mathcal{G} and the trace of the energy-momentum tensor T , κ denotes the coupling constant, g is for the determinant of the metric tensor, R is the Ricci Scalar, and \mathcal{L}_M represents matter part of the Lagrangian. The Gauss-Bonnet term \mathcal{G} is defined as

$$\mathcal{G} = R^2 - 4R_{\zeta\eta}R^{\zeta\eta} + R_{\zeta\eta\mu\nu}R^{\zeta\eta\mu\nu}, \quad (4)$$

where $R_{\zeta\eta\mu\nu}$, and $R_{\zeta\eta}$ is the Reimann and Ricci tensors, respectively. The variation of Eq.(3) with respect to $g_{\zeta\eta}$, and by setting $\kappa = 1$, gives the following fourth order non-linear field equations

$$\begin{aligned} G_{\zeta\eta} = & [2Rg_{\zeta\eta}\nabla^2 + 2R\nabla_{\zeta}\nabla_{\eta} + 4g_{\zeta\eta}R^{\mu\nu}\nabla_{\mu}\nabla_{\nu} + 4R_{\zeta\eta}\nabla^2 - \\ & 4R_{\zeta}^{\mu}\nabla_{\eta}\nabla_{\mu} - 4R_{\eta}^{\mu}\nabla_{\zeta}\nabla_{\mu} - 4R_{\zeta\mu\eta\nu}\nabla^{\mu}\nabla^{\nu}]f_{\mathcal{G}} + \frac{1}{2}g_{\zeta\eta}f - [T_{\zeta\eta} + \Theta_{\zeta\eta}] \times \\ & f_T - [2RR_{\zeta\eta} - 4R_{\zeta}^{\mu}R_{\mu\eta} - 4R_{\zeta\mu\eta\nu}R^{\mu\nu} + 2R_{\zeta}^{\mu\nu\delta}R_{\eta\mu\nu\delta}]f_{\mathcal{G}} + \kappa^2 T_{\zeta\eta}, \quad (5) \end{aligned}$$

where $\square = \nabla^2 = \nabla_{\zeta}\nabla^{\zeta}$ is the d'Alembertian operator, $G_{\zeta\eta} = R_{\zeta\eta} - \frac{1}{2}g_{\zeta\eta}R$ is the Einstein tensor, $\Theta_{\zeta\eta} = g^{\mu\nu}\frac{\delta T_{\mu\nu}}{\delta g_{\zeta\eta}}$, $f \equiv f(\mathcal{G}, T)$, $f_{\mathcal{G}} \equiv \frac{\partial f(\mathcal{G}, T)}{\partial \mathcal{G}}$, and $f_T \equiv \frac{\partial f(\mathcal{G}, T)}{\partial T}$. Einstein equations can be reawakened by putting simply $f(\mathcal{G}, T) = 0$ whereas field equations for $f(\mathcal{G})$ are reproduced by replacing $f(\mathcal{G}, T)$ with $f(\mathcal{G})$ in Eq.(5). The energy-momentum tensor denoted by $T_{\zeta\eta}$ can be defined as

$$T_{\zeta\eta} = -\frac{2}{\sqrt{-g}}\frac{\delta(\sqrt{-g}\mathcal{L}_M)}{\delta g^{\zeta\eta}}. \quad (6)$$

Moreover, the metric dependent energy-momentum tensor may have the form

$$T_{\zeta\eta} = g_{\zeta\eta}\mathcal{L}_M - 2\frac{\partial \mathcal{L}_M}{\partial g^{\zeta\eta}}. \quad (7)$$

The usual anisotropic energy momentum tensor $T_{\zeta\eta}$ is given as

$$T_{\zeta\eta} = (\rho + p_t)V_{\zeta}V_{\eta} - p_t g_{\zeta\eta} + (p_r - p_t)\xi_{\zeta}\xi_{\eta}, \quad (8)$$

where p_t and p_r represents the tangential and radial pressures respectively while ρ denotes the energy density. The four velocity is denoted by V_{ζ} and the radial four vector by ξ_{α} , satisfying

$$V^{\alpha} = e^{\frac{-a}{2}}\delta_0^{\alpha}, \quad V^{\alpha}V_{\alpha} = 1, \quad \xi^{\alpha} = e^{\frac{-b}{2}}\delta_1^{\alpha}, \quad \xi^{\alpha}\xi_{\alpha} = -1. \quad (9)$$

In this paper, we have chosen specifically the following $f(\mathcal{G}, T)$ model [49]

$$f(\mathcal{G}, T) = f_1(\mathcal{G}) + f_2(T), \quad (10)$$

where $f_1(\mathcal{G})$ is an analytic function comprised of Gauss-Bonnet term. In particular, we consider $f_1(\mathcal{G}) = \alpha\mathcal{G}^n$, a power law model of $f(\mathcal{G})$ gravity proposed by Cognola et al. [51] with α being an arbitrary real constant, and n a positive real number. Here we take $f_2(T) = \lambda T$, with λ being some positive real number. Further, for the investigations on the compact stars we take the static, spherically symmetric space-time as

$$ds^2 = e^{a(r)} dt^2 - e^{b(r)} dr^2 - r^2 d\theta^2 - r^2 \sin^2\theta d\phi^2. \quad (11)$$

We parameterize metric (11) by taking $a(r) = Br^2 + C$ and $b(r) = Ar^2$, given by Krori and Barua [15] and with the help of some physical assumptions, the arbitrary constants A, B and C will be calculated. The above set of functions are established to reach a singularity free structure for compact stars. Therefore, our main concern is to present these functions to the metric in a way to achieve the structure for the compact star under this extended model, free from the singularities in the neighbourhood of r . To investigate the existence of the compact stars for the model $f(\mathcal{G}, T) = \alpha\mathcal{G}^n + \lambda T$, we have considered $\alpha = 1$, $\lambda = 2$, and $n = 2$. For these parametric values, the energy density and all the energy conditions remain positive for the model under investigation. It is worth mentioning here that one may opt for some other choices of these values for further analysis. The explicit expressions for the energy density ρ , radial pressure p_r , and the tangential pressure p_t are

obtained as

$$\begin{aligned}
\rho = & \frac{e^{-2b}}{8r^4(1+\lambda)(1+2\lambda)} \left[8e^b(-1+e^b)r^2(1+2\lambda) - 4e^{2b}r^4(1+\lambda)f_1 \right. & (12) \\
& + f_G \left\{ -16(-1+e^b)^2\lambda + r^2 \left\{ r^2(1+2\lambda)a^4 - 2r^2(1+2\lambda)a^3b' \right. \right. \\
& - 4a'b' \left\{ 2(-3+e^b)(1+\lambda) + r^2(1+2\lambda)a'' + a'^2 \left\{ 8(\lambda+e^b(1+\lambda)) \right\} \right. \\
& + r^2(1+2\lambda)(b'^2+4a'') \left. \right\} + 4 \left\{ -2\lambda b'^2 + a'' \left\{ 4(-1+e^b)(1+\lambda) \right\} \right. \\
& + r^2(1+2\lambda)a'' \left. \right\} \left. \right\} + 2r \left\{ 4f'_G \left\{ -8(2+5\lambda) + r \left\{ b'(10+27\lambda-2r\lambda b') \right\} \right. \right. \\
& - r \left\{ 8+18\lambda + r(2+3\lambda)b' \right\} a'' \left. \right\} - 8r(2+5\lambda)(1-2rb'+r^2a'')f''_G \\
& + r^2a'^2 \left\{ e^br\lambda - 2(8+18\lambda+r(2+3\lambda)b')f'_G - 4r(2+5\lambda)f''_G \right\} \\
& + 2e^b \left\{ 16(2+5\lambda)f'_G + 2rb' \left\{ r+2r\lambda + (2+3\lambda)f'_G \right\} + r^3\lambda a'' + 4r(2+5\lambda)f''_G \right\} \\
& + ra' \left\{ 2(-32-74\lambda+rb'(2\lambda+r(2+3\lambda)b')) \right\} f'_G - e^b\lambda \left\{ r(-4+rb') + 4f'_G \right\} \\
& + 4r \left\{ -2(4+9\lambda) + r(2+5\lambda)b'f''_G \right\} \left. \right\},
\end{aligned}$$

$$\begin{aligned}
p_r = & \frac{e^{-2b}}{8r^4(1+\lambda)(1+2\lambda)} \left[-4e^{2b}r^4(1+\lambda)f_1 + f_G \left\{ -16(-1+e^b)^2\lambda \right. \right. & (13) \\
& + r^2 \left(r^2(1+2\lambda)a^4 - 2r^2(1+2\lambda)a^3b' - 4a'b' \left\{ 2(-3+e^b)(1+\lambda) \right. \right. \\
& + r^2(1+2\lambda)a'' \left. \right\} + a'^2 \left\{ 8(-1+e^b)(1+\lambda) + r^2(1+2\lambda)(b'^2+4a'') \right\} \\
& + 4 \left\{ 2(1+\lambda)b'^2 + a'' \left\{ 4(-1+e^b)(1+\lambda) + r^2(1+2\lambda)a'' \right\} \right\} \left. \right\} \\
& + 2r \left\{ 4e^b(-1+e^b) \right\} r(1+2\lambda) + 4f'_G \left\{ -8\lambda + r \left\{ -b'(4+\lambda+2r\lambda b') \right. \right. \\
& + r\lambda(-2+rb'a'') + r^2\lambda a'^2 \left\{ 2(-2+rb')f'_G + r(e^b-4f''_G) \right\} - 8r\lambda(1-2rb' \\
& + r^2a'')f''_G + ra' \left\{ -2 \left\{ 12+34\lambda + rb'(8+14\lambda+r\lambda b') \right\} f'_G \right. \\
& + e^b \left\{ -r(4+4\lambda+r\lambda b') + 4(2+3\lambda)f'_G \right\} + 4r\lambda(-2+rb')f''_G \left. \right\} \\
& + 2e^b \left[2 \left\{ 8\lambda + r(4+7\lambda)b' \right\} f'_G + r\lambda(r^2a'' + 4f''_G) \right] \left. \right\},
\end{aligned}$$

$$\begin{aligned}
p_t = & \frac{e^{-2b}}{4r^4(1+\lambda)(1+2\lambda)} \left[-2e^{2b}r^4(1+\lambda)f_1 + 2f_{\mathcal{G}} \left\{ 4(-1+e^b)^2(1+\lambda) \right. \right. \\
& + r^2 \left\{ \{-1+2e^b(1+\lambda)\}a'^2 - 2(-3+e^b)(1+\lambda)a'b' + b'^2 + 4(-1+e^b)(1 \right. \\
& + \left. \left. \lambda\}a'' \right\} \right] - r \left\{ 4f'_{\mathcal{G}} [8\lambda + r\{b'(-7\lambda - 2r(1+\lambda)b') + r(2+6\lambda \right. \\
& + r(2+3\lambda)b')a''] + 8r\lambda(1-2rb' + r^2a'')f''_{\mathcal{G}} + 2e^b\{-16\lambda f'_{\mathcal{G}} - rb'(r+2r\lambda \\
& - 2\lambda f'_{\mathcal{G}}) + r^3(1+\lambda)a'' - 4r\lambda f''_{\mathcal{G}}\} + r^2a'^2 \left\{ e^br(1+\lambda) + 2 \left\{ 2+6\lambda \right. \right. \\
& + r(2+3\lambda)b' \left. \left. \right\} f'_{\mathcal{G}} + 4r\lambda f''_{\mathcal{G}} \right\} + ra' - 2[-10\lambda + rb'\{2+6\lambda \\
& + r(2+3\lambda)b'\}]f'_{\mathcal{G}} + e^b[-r\{-2+r(1+\lambda)b'\} + 4\lambda f'_{\mathcal{G}}] + 4r(2+6\lambda - r\lambda b')f''_{\mathcal{G}} \left. \right\} \right], \tag{14}
\end{aligned}$$

where prime denotes the radial derivative.

3 Matching With Schwarzschild's Exterior Metric

Whatever the geometry of the star is, either derived internally or externally, the intrinsic boundary metric remains the same. Thus, confirming that the components of the metric tensor irrespective of the coordinate system across the surface of the boundary will remain continuous. No doubt, in GR, the Schwarzschild solutions have been pioneer in guiding us to choose from the diverse possibilities of the matching conditions while investigating the stellar compact objects. Now when we come to the case of modified theories of gravity, modified TOV equations with zero pressure and energy density, the solution outside the star can differ from Schwarzschild's solution. However, it is expected that the solutions of the modified TOV equations with energy density and pressure (may be non-zero) may accommodate Schwarzschild's solution with some specific choice of $f(\mathcal{G}, T)$ gravity model. Perhaps this is the reason that Birkhoff's theorem may not hold in modified gravity. The detailed investigation of the issue in the context of $f(\mathcal{G}, T)$ gravity can be an interesting task. Many authors have considered Schwarzschild solution for this purpose giving some interesting results [52]-[55]. Now to solve the field equations under the restricted boundary conditions at $r = R$, the pressure $p_r = 0$, the interior metric (11) requires these matching conditions. This can be done by taking a smooth match at $r = R$ to Schwarzschild's exterior

metric, given by

$$ds^2 = \left(1 - \frac{2M}{r}\right) dt^2 - \left(1 - \frac{2M}{r}\right)^{-1} dr^2 - r^2(d\theta^2 + \sin^2\theta d\phi^2), \quad (15)$$

yielding

$$g_{tt}^- = g_{\alpha}^+, \quad g_{rr}^- = g_{rr}^+, \quad \frac{\partial g_{\alpha}^-}{\partial r} = \frac{\partial g_{\alpha}^+}{\partial r}, \quad (16)$$

where (+) corresponds to exterior solution and (-) to the interior solution. Now from the comparison of exterior and interior metrics, the constants A , B , and C are obtained as

$$A = \frac{-1}{R^2} \ln\left(1 - \frac{2M}{R}\right), \quad (17)$$

$$B = \frac{M}{R^3} \left(1 - \frac{2M}{R}\right), \quad (18)$$

$$C = \ln\left(1 - \frac{2M}{R}\right) - \frac{M}{R} \left(1 - \frac{2M}{R}\right). \quad (19)$$

The approximated values of the mass M and radius R of the compact stars Her X-1, SAX J1808.4-3658 and 4U1820-30 are used to calculate the values of constants A and B [56, 57]. The result $\mu = \frac{M(R)}{R}$ defines the compactness of the star and the expression $Z_s = (1 - 2\mu)^{-1/2} - 1$ determines the surface redshift Z_s . For the compact stars under consideration, the values of Z_s have been given below in table as follows.

Compact Stars	M	$R(km)$	$\mu = \frac{M}{R}$	$A(km^{-2})$	$B(km^{-2})$	Z_s
Her X-1	$0.88M_{\odot}$	7.7	0.168	0.006906276428	0.004267364618	0.23
SAXJ1808.4-3658	$1.435M_{\odot}$	7.07	0.299	0.01823156974	0.01488011569	0.57
4U1820-30	$2.25M_{\odot}$	10.0	0.332	0.01090644119	0.009880952381	0.73

Table 1: The approximate values of the masses M , radii R , compactness μ , and the constants A , and B for the compact stars Her X-1, SAXJ 1808.4-3658, and 4U 1820-30

Now making use of Krori and Barua metric, Eqs. (12)-(14) take the form

$$\begin{aligned}
\rho = & \frac{e^{-2Ar^2}}{2r^4(1+\lambda)(1+2\lambda)} \left[4 \left\{ -\lambda - e^{2Ar^2}\lambda + 2e^{Ar^2} \{ \lambda + Br^2(1 \right. \right. \quad (20) \\
& + (-A+B)r^2)(1+\lambda) + r^2 \{ -2A^2r^2\lambda + 2B(-1+3Ar^2)(1+\lambda) \\
& + B^4r^6(1+2\lambda) - 2B^3r^4(-1+Ar^2)(1+2\lambda) + B^2r^2(1+4\lambda \\
& + Ar^2(-2+Ar^2)(1+2\lambda) \} \} \} f_G + r \left\{ -4(2+5\lambda) + r^2(10A-24B \right. \\
& - 4B(A+2B)r^2 + 4A(A-B)Br^4 + \{ 27A-55B-2(2A^2+2AB \\
& + 9B^2)r^2 + 6A(A-B)Br^4 \} \lambda) + e^{Ar^2} [8+20\lambda + r^2(-B\lambda + A(2 \\
& + 3\lambda))] f'_G + r(e^{Ar^2}(-2+4Ar^2-4\lambda+2r^2(4A+3B+B(-A \\
& + B)r^2)\lambda + e^{Ar^2}(2+4\lambda-8^n r^2 \\
& \times \frac{1}{r^{2n}} (Be^{-2Ar^2}(1+(-3A+B)r^2 + e^{Ar^2}(-1+(A-B)r^2)))^n \\
& \times \alpha(1+\lambda)) + 4(-2-5\lambda + e^{Ar^2}(2+5\lambda) + 2r^2(A(2+Br^2)(2+5\lambda) \\
& - B(6+14\lambda+Br^2(2+5\lambda)))) f''_G \left. \right\} \right],
\end{aligned}$$

$$\begin{aligned}
p_r = & \frac{e^{-2Ar^2}}{2r^4(1+\lambda)(1+2\lambda)} \left[4 \left\{ -(-1+e^{Ar^2})^2\lambda + 2A^2r^4(1+\lambda) \right. \quad (21) \\
& - 2Br^2(1-3Ar^2 + e^{Ar^2}(-1+Ar^2))(1+\lambda) + B^4r^8(1+2\lambda) \\
& - 2B^3r^6(-1+Ar^2)(1+2\lambda) + B^2r^4(-1+2e^{Ar^2}(1+\lambda) + Ar^2(-2 \\
& + Ar^2)(1+2\lambda)) \left. \right\} f_G + r(e^{Ar^2}r(e^{Ar^2}(2+4\lambda-8^n r^2 \\
& \times \frac{1}{r^{2n}} (Be^{-2Ar^2}(1+(-3A+B)r^2 + e^{Ar^2}(-1+(A-B)r^2)))^n \\
& \times \alpha(1+\lambda)) - 2(1+2\lambda+Br^2(2+(1+(A-B)r^2)\lambda))) \\
& + 4(-4\lambda-r^2(4A+6B+8ABr^2+(A+19B+2(2A^2+6AB+B^2)r^2 \\
& + 2A(A-B)Br^4)\lambda) + e^{Ar^2}(4\lambda+r^2(B(2+3\lambda)+A(4+7\lambda)))) f'_G \\
& + 4r(-1+e^{Ar^2}+2(A-B)r^2(2+Br^2))\lambda f''_G \left. \right],
\end{aligned}$$

$$\begin{aligned}
p_t &= \frac{e^{-2Ar^2}}{2r^4(1+\lambda)(1+2\lambda)} \left[4(1+A^2r^4-B^2r^4+\lambda+e^{2Ar^2}(1+\lambda)) \right. \\
&+ 2Br^2(-1+3Ar^2)(1+\lambda) + 2e^{Ar^2}(-1+Br^2+B(-A+B)r^4) \\
&\times (1+\lambda) f_{\mathcal{G}} + r(e^{Ar^2}r^3(-8^n e^{Ar^2} \times \frac{1}{r^{2n}} (Be^{-2Ar^2}(1+(-3A+B)r^2 \\
&+ e^{Ar^2}(-1+(A-B)r^2)))^n \alpha(1+\lambda) - 2B(2+\lambda+Br^2(1+\lambda)) + 2A \\
&\times (1+2\lambda+Br^2(1+\lambda))) + 4(4(-1+e^{Ar^2})\lambda + r^2(A(-(-7+e^{Ar^2})\lambda \\
&+ 4Ar^2(1+\lambda)) - 2B^2r^2(1+3\lambda+Ar^2(2+3\lambda)) + B(-2-(11+e^{Ar^2}))\lambda \\
&+ 2Ar^2(-1+Ar^2(2+3\lambda)))) f'_{\mathcal{G}} - 4r(\lambda - e^{Ar^2}\lambda + 2r^2(B-2A\lambda \\
&+ B(4+(-A+B)r^2)\lambda)) f''_{\mathcal{G}} \left. \right], \tag{22}
\end{aligned}$$

where (23)

$$\begin{aligned}
f_1 &= \alpha \left[\frac{e^{-2Ar^2}(-16ABr^2 + 2(1 - e^{Ar^2})(4B - 4ABr^2 + 4B^2r^2))}{r^2} \right]^n, \\
f'_{\mathcal{G}} &= \frac{1}{r^3} \left[2^{-2+3n} Be^{-2Ar^2} (-1+n)n (Be^{-2Ar^2}(1+(-3A+B)r^2) \right. \\
&+ e^{Ar^2}(-1+(A-B)r^2)) r^{2-2+n} (-1+6A^2r^4 - 2A(r^2+Br^4) \\
&+ e^{Ar^2}(1+Ar^2+A(-A+B)r^4)) \alpha \left. \right], \tag{24}
\end{aligned}$$

$$\begin{aligned}
f''_{\mathcal{G}} &= \frac{4^{-1+2n} e^{3Ar^2} (-1+n)n \alpha}{B(-1+(3A-B)r^2 + e^{Ar^2}(1+(-A+B)r^2))^3} \tag{25} \\
&\times \frac{1}{r^{2n}} \left(-Be^{-\frac{3Ar^2}{2}} (Ar^2 \cosh(\frac{Ar^2}{2})) + (1+(2A+B)r^2) \sinh(\frac{Ar^2}{2}) \right)^n \\
&\times (2-4n-3(2B+A(-9+4n))r^2 + 2A(9B-6Bn+A(-21+10n))r^4 \\
&+ A(3B^2-16ABn+A^2(-15+32n))r^6 - 2A^2(3A^2-4AB+B^2) \\
&\times (-3+4n)r^8 + (-2+4n+3(2B+A(-9+4n))r^2 + 2A(16A-9B \\
&- 9An+6Bn)r^4 + A(-3B^2+A^2(33-52n)+2AB(-3+10n))r^6 \\
&+ 2A^2(37A^2-26AB+5B^2)(-1+n)r^8) \cosh(Ar^2) + Ar^2(11-4n \\
&+ 2(B(3-2n)+A(-12+7n))r^2 + (B^2+2AB(1-6n)+A^2(-27 \\
&+ 44n))r^4 - 2A(7A-3B)(5A-B)(-1+n)r^6) \sinh(Ar^2).
\end{aligned}$$

Now we investigate the nature and some interesting features of the compact star, specifically for the assumed model of $f(\mathcal{G}, T)$ gravity.

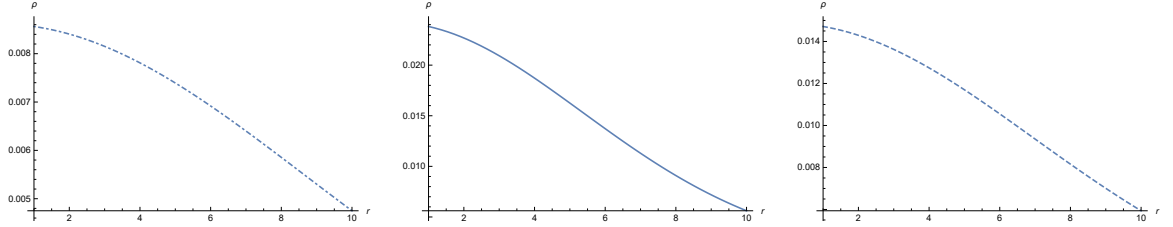


Figure 1: Plot of the density evolution of the strange star candidate Her X-1, SAX J 1808.4-3658, and 4U 1820-30; represented by (left to right) 1st, 2nd, and 3rd graphs, respectively.

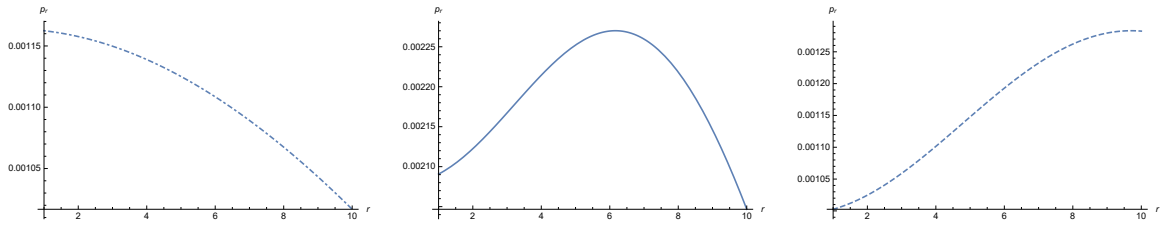


Figure 2: Plots of the radial pressure evolution of the strange star candidates Her X-1, SAX J 1808.4-3658, and 4U 1820-30; represented by (left to right) 1st, 2nd, and 3rd graphs, respectively.

4 Physical Aspects of $f(\mathcal{G}, T)$ Gravity Model

In this section, some interesting physical aspects of the compact stars such as the energy density and pressure evolutions, energy conditions, equilibrium conditions, stability and adiabatic index analysis, compactness, and redshift analysis shall be discussed.

4.1 Energy Density and Pressure Evolutions

The plot of the energy density for the strange star candidate Her X-1 (Figure 1) shows that as $r \rightarrow 0$, ρ goes to maximum, and this in fact indicates the high compactness of the core of the star validating that our model under

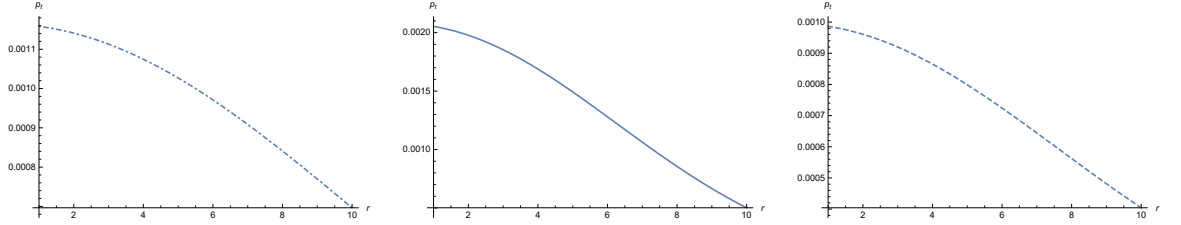


Figure 3: Plots of the transverse pressure evolution of the strange star candidates Her X-1, SAX J 1808.4-3658, and 4U 1820-30; represented by (left to right) 1st, 2nd, and 3rd graphs, respectively.

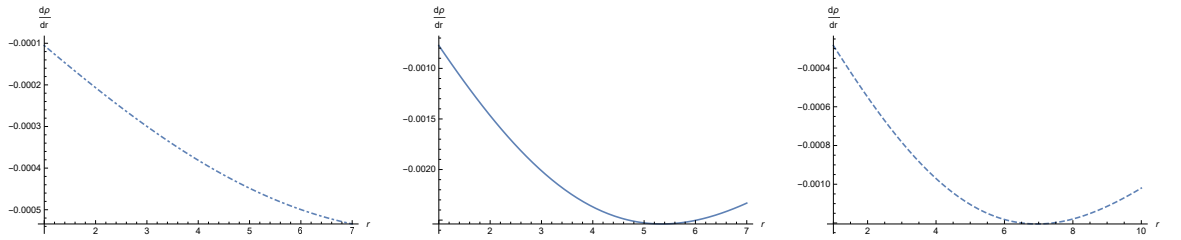


Figure 4: Plots of $\frac{d\rho}{dr}$ with increasing radius of the strange star candidates Her X-1, SAX J 1808.4-3658, and 4U 1820-30; represented by (left to right) 1st, 2nd, and 3rd graphs, respectively.

investigation is viable for the outer region of the core. The other two graphs in the same row provide us with similar sort of conclusions. Furthermore, from the other plots of the anisotropic radial pressure p_r (Figure 2), it is evident that the radius of the star for this model is $R = 10$ km which further when used, gives us the density of $1.5828 \times 10^{15} \text{ g cm}^{-3}$, a high value with a small radius of 10 km, showing that our $f(\mathcal{G}, T)$ model is compatible to the structure of ultra-compact star [10, 59]. A comparison of this with the already existing data, labels this compact star as quark/strange star [60]. All the three plots in Figure (3) indicate that the tangential pressure p_t remains positive and finite and show their decreasing behavior, which is required for the viability of the compact star model.

The variations of the radial derivatives of the density and radial pressure

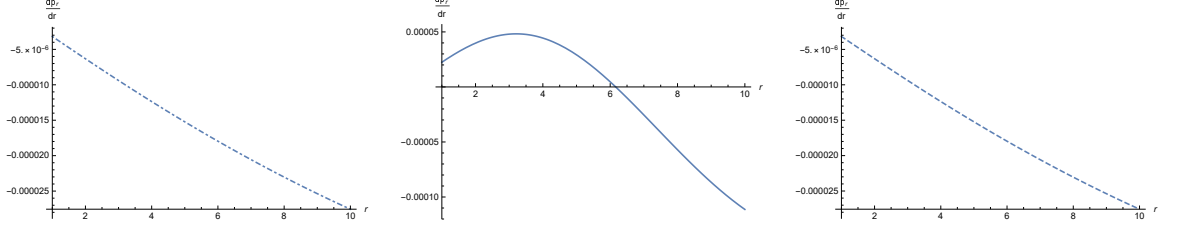


Figure 5: Variations of $\frac{dp_r}{dr}$ with increasing radius of the strange star candidate Her X-1, SAX J 1808.4-3658, and 4U 1820-30; represented by (left to right) 1st, 2nd, and 3rd graphs, respectively.

are shown in Figures (4) and (5) respectively. One can see the decreasing evolution of the first r -derivatives i.e $\frac{d\rho}{dr} < 0$ and $\frac{dp_r}{dr} < 0$. It may be noted here that at $r = 0$, these derivatives just disappear except of the radial pressure for the SAX J 1808.4-3658 candidate. The mathematical calculations for the second derivative test both for ρ and p_r tell us that $\frac{d^2\rho}{dr^2} < 0$ and $\frac{d^2p_r}{dr^2} < 0$, indicating the maximum values of the density and radial pressure at the center. This further suggests the compact nature of the star.

4.2 Energy Conditions

For the viability of the model, the energy bounds must be satisfied due to their significant importance in analysing the theoretical data. NEC (null energy conditions), WEC (weak energy conditions), SEC (strong energy conditions), and DEC (dominant energy conditions) have been given as

$$\begin{aligned}
 \mathbf{NEC} & : \quad \rho + p_r \geq 0, \quad \rho + p_t \geq 0, \\
 \mathbf{WEC} & : \quad \rho \geq 0, \quad \rho + p_r \geq 0, \quad \rho + p_t \geq 0, \\
 \mathbf{SEC} & : \quad \rho + p_r \geq 0, \quad \rho + p_t \geq 0, \quad \rho + p_r + 2p_t \geq 0, \\
 \mathbf{DEC} & : \quad \rho > |p_r|, \quad \rho > |p_t|.
 \end{aligned}$$

The evolution of all these energy conditions have been well satisfied as represented graphically for the strange star candidate Her X-1 in Figure (6). Hence our solutions are physically viable.

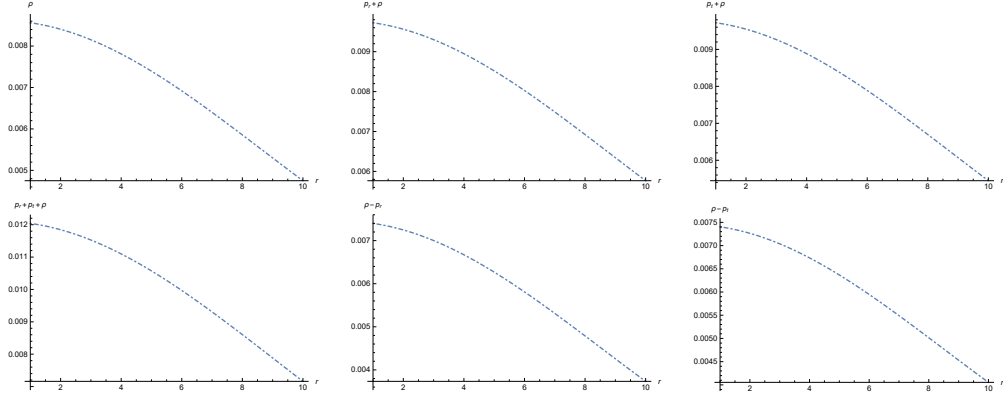


Figure 6: Plots of energy conditions with respect to radius r (km) of the strange star candidate Her X-1.

4.3 Tolman-Oppenheimer-Volkoff (TOV) Equation

In anisotropic case, the generalized TOV equation is given as

$$\frac{M_G(r)(\rho + p_r)}{r^2} e^{\frac{b-a}{2}} + \frac{dp_r}{dr} - \frac{2}{r}(p_t - p_r) = 0, \quad (26)$$

where

$$M_G(r) = \frac{1}{2} r^2 e^{\frac{a-b}{2}} a' \quad (27)$$

is the gravitational mass of a sphere of radius r . Now putting Eq.(27) into Eq.(26), it follows

$$-\frac{a'}{2}(\rho + p_r) - \frac{dp_r}{dr} + \frac{2}{r}(p_t - p_r) = 0. \quad (28)$$

Eq.(28) gives the information about the stellar configuration equilibrium under the combined effect of different forces like the anisotropic force F_a , the hydrostatic force F_h , and the gravitational force F_g . Their summation to zero eventually describes the equilibrium condition of the form

$$F_g + F_h + F_a = 0, \quad (29)$$

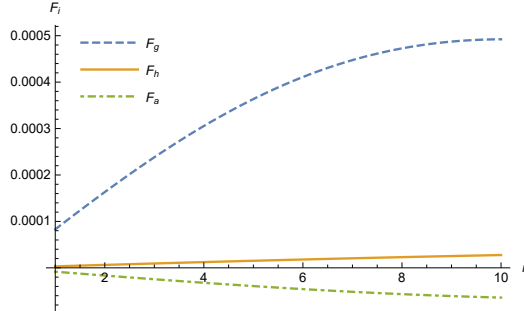


Figure 7: The plot of gravitational force (F_g), hydrostatic force (F_h) and anisotropic force (F_a) for the strange star candidate Her X-1 with respect to the radial coordinate r (km).

where

$$\begin{aligned}
 F_g &= -\frac{a'}{2}(\rho + p_r), \\
 F_h &= -\frac{dp_r}{dr}, \\
 F_a &= \frac{2}{r}(p_t - p_r).
 \end{aligned}
 \tag{30}$$

From Figure (7), it can be noticed that under the mutual effect of the three forces F_g , F_h and F_a , the static equilibrium might be achieved. It is mentioned here that at some point if $p_r = p_t$ then $F_a = 0$, which suggests that the equilibrium becomes independent of the anisotropic force F_a .

4.4 Stability Analysis

For the stability, the radial and transversal sound speeds denoted by v_{sr}^2 and v_{st}^2 respectively, should satisfy the bounds, $0 \leq v_{sr}^2 \leq 1$ and $0 \leq v_{st}^2 \leq 1$ [61], where $\frac{dp_r}{d\rho} = v_{sr}^2$ and $\frac{dp_t}{d\rho} = v_{st}^2$. It can be seen from the Figures (8) and (9) that the evolution of the radial and transversal sound speeds for strange star candidate Her X-1 are within the bounds of stability as discussed, but in the case of SAX J 1808.4-3658, and 4U 1820-30 strange star candidates, the radial sound speeds evolution which is against the radial coordinate r temporarily violates these stability conditions. However, for the same candidates the

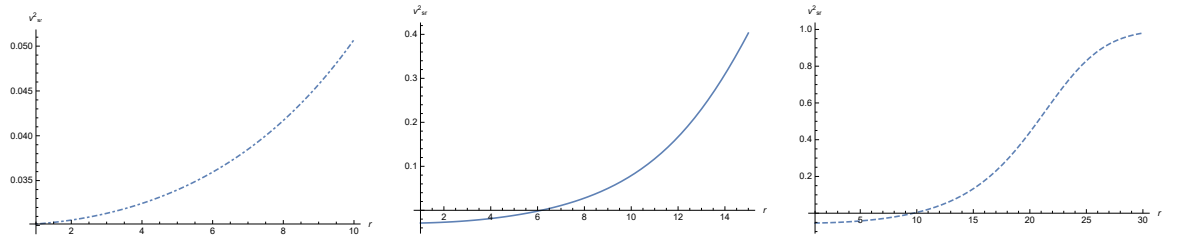


Figure 8: Variations of v_{sr}^2 with respect radius r (km) of the strange star candidate Her X-1, SAX J 1808.4-3658, and 4U 1820-30; represented by (left to right) 1st, 2nd, and 3rd graphs, respectively.

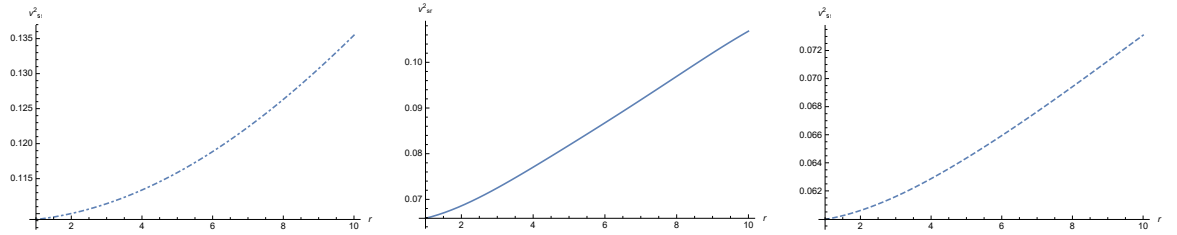


Figure 9: Variations of v_{st}^2 with respect radius r (km) of the strange star candidate Her X-1, SAX J 1808.4-3658, and 4U 1820-30; represented by (left to right) 1st, 2nd, and 3rd graphs, respectively.

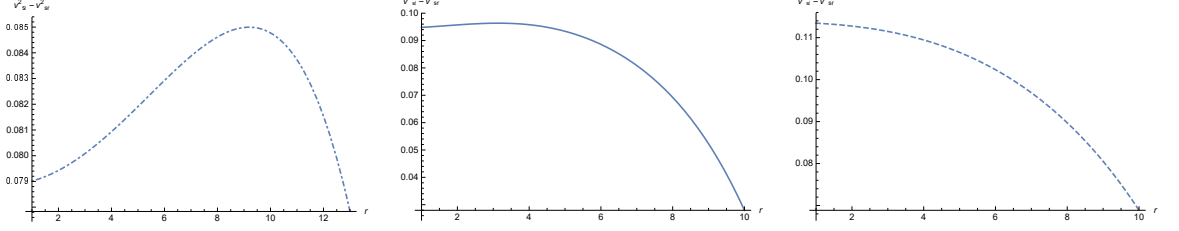


Figure 10: Variations of $v_{st}^2 - v_{sr}^2$ with respect to radius r (km) of the strange star candidate Her X-1, SAX J 1808.4-3658, and 4U 1820-30; represented by (left to right) 1st, 2nd, and 3rd graphs, respectively.

transversal sound speeds are satisfied. Within the matter distribution, the estimation of the potentially stable and unstable eras can be had from the differences of the propagations of the sound speeds which is the expression $v_{st}^2 - v_{sr}^2$ satisfying the inequality $0 < |v_{st}^2 - v_{sr}^2| < 1$. This can be seen clearly from the plots of Figure (10). Thus, overall the stability may be attained for compact stars under $f(\mathcal{G}, T)$ gravity model, particularly for the strange star candidate Her X-1.

4.5 Adiabatic Index Analysis

For the case of anisotropic fluid spherical star, as proposed in [62, 63], the stability depends on the adiabatic index γ , and for the radial and tangential cases, we respectively have

$$\gamma_r = \frac{\rho + p_r}{p_r} \frac{dp_r}{d\rho} \quad \text{and} \quad \gamma_t = \frac{\rho + p_t}{p_t} \frac{dp_t}{d\rho}. \quad (31)$$

The stability of a Newtonian sphere should be satisfied if $\gamma > \frac{4}{3}$, and $\gamma = \frac{4}{3}$ is the condition for the occurrence of neutral equilibrium [64]. Due to the presence of the effective pressure, the anisotropic relativistic sphere obeys more complicated stability condition given as

$$\gamma > \frac{4}{3} + \left[\frac{4 p_{t0} - p_{r0}}{3 |p'_{r0}| r} + \frac{8\pi \rho_0 p_{r0} r}{3 |p'_{r0}|} \right]_{max}, \quad (32)$$

where ρ_0 , p_{t0} , and p_{r0} are the initial energy density, tangential pressure, and radial pressure in static equilibrium respectively satisfying Eq. (26). In our

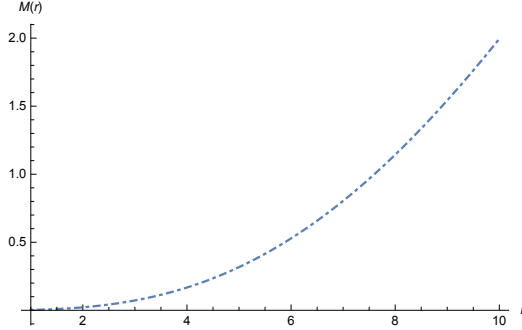


Figure 11: Evolution of mass-function $M(r)$ for the strange star candidate Her X-1 with respect to the radial coordinate r (km).

case, the adiabatic index has been calculated analytically for strange star candidate Her X-1, giving us $\gamma_r = 1.3757$ and $\gamma_t = 1.0597$, which shows the complete stability in radial case but some deviation in the tangential case.

4.6 Mass-Radius Relationship

The mass of the compact star as a function of radius r is given as

$$M(r) = 4 \int_0^r \pi r'^2 \rho dr'. \quad (33)$$

It can be seen clearly from the profile of the mass function given in Figure (11) that the mass of the star is directly proportional to the radius, and $M(r) \rightarrow 0$ as $r \rightarrow 0$, which depicts that the mass function is regular at the centre of the star. Moreover, for the spherically symmetric anisotropic perfect fluid case, the ratio of the mass to the radius, according to Buchdahl [6] should be bounded like $\frac{2M}{r} \leq \frac{8}{9}$. In our case, the situation is very good as we get $\frac{2M}{r} = 0.4987$ and the condition is clearly satisfied.

4.7 Compactness and Redshift Analysis

Compactness $\mu(r)$ of the star is expressed as

$$\mu(r) = \frac{4}{r} \int_0^r \pi r'^2 \rho dr'. \quad (34)$$

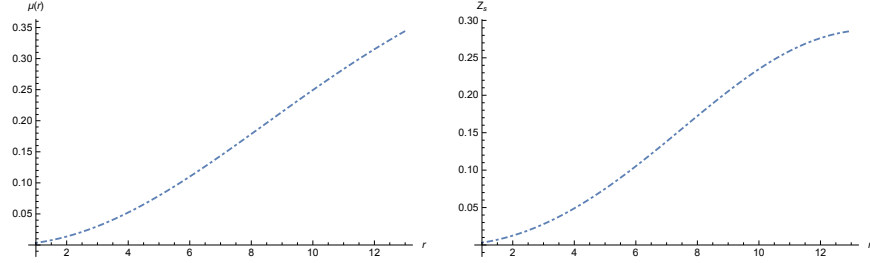


Figure 12: Plots of the Compactness $\mu(r)$ and Surface redshift (Z_s) of the strange star candidate Her X-1 with respect to the radial coordinate r (km).

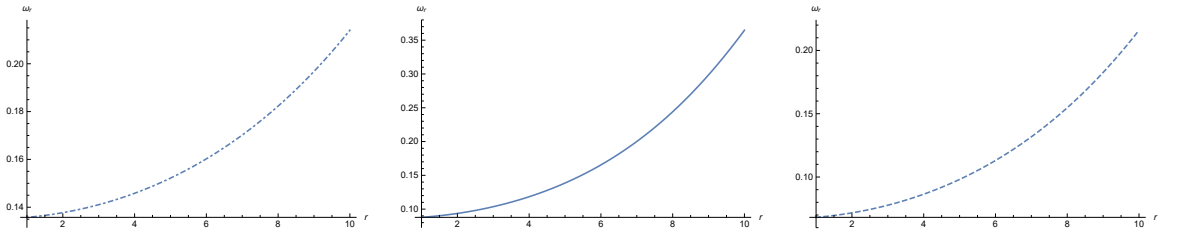


Figure 13: Variations of the radial EoS parameter with respect to the radial coordinate r (km) of the strange star candidate Her X-1, SAX J 1808.4-3658, and 4U 1820-30; represented by (left to right) 1st, 2nd, and 3rd graphs, respectively.

Therefore, the redshift Z_S is determined as

$$Z_S + 1 = [-2\mu(r) + 1]^{-\frac{1}{2}}. \quad (35)$$

The graphical evolution of the surface redshift has been given in Figure (12). The value of the function Z_S for the case of the strange star candidate Her X-1 is calculated as $Z_S \approx 0.22$ which is within the desired bound of $Z_S \leq 2$.

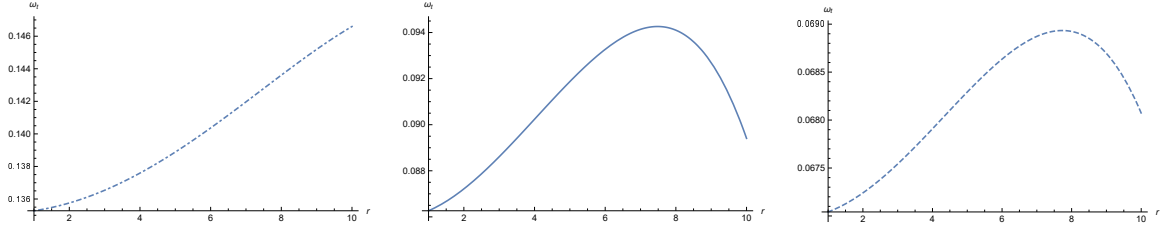


Figure 14: Variations of the tangential EoS parameter with respect to the radial coordinate r (km) of the strange star candidate Her X-1, SAX J 1808.4-3658, and 4U 1820-30; represented by (left to right) 1st, 2nd, and 3rd graphs, respectively.

4.8 EoS Parameter and the Measurement of Anisotropy

Now for anisotropic case, the radial and transversal forms of EoS parameter can be written as

$$\omega_r = \frac{p_r}{\rho} \quad \text{and} \quad \omega_t = \frac{p_t}{\rho}. \quad (36)$$

The evolution of these EoS parameters with the increasing radius have been shown in Figures (13 and 14) which clearly demonstrate that all the six plots satisfy the inequalities $0 < \omega_r < 1$ and $0 < \omega_t < 1$. This further advocates the effectiveness of the considered model.

The measurement of the anisotropy denoted by Δ is given by

$$\Delta = \frac{2}{r}(p_t - p_r), \quad (37)$$

which gives the information about the anisotropic behavior of the model. The Δ remains positive if $p_t > p_r$, suggesting the anisotropy being drawn outward, and for the reverted situation, i.e., $p_t < p_r$, the anisotropy Δ turns negative which corresponds to being directed inward. For our situation, the variations of the anisotropic measurement Δ with respect to the radial coordinate r show the decreasing negative behavior for the strange star candidate Her X-1 and SAX J 1808.4-3658 suggesting that $p_t < p_r$. For the 4U 1820-30 candidate, it remains positive for a fraction of the radius r where some repulsive anisotropic force followed by massive matter distribution appears and very soon, it gets negative after $r = 0.25$.

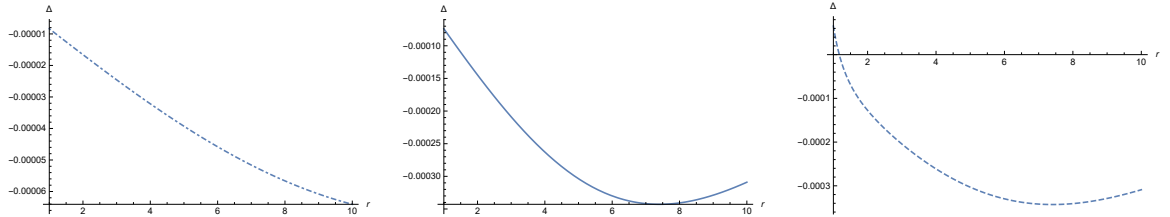


Figure 15: Variations of anisotropic measure Δ with respect to the radial coordinate r (km) of the strange star candidate Her X-1, SAX J 1808.4-3658, and 4U 1820-30; represented by (left to right) 1st, 2nd, and 3rd graphs, respectively.

5 Concluding Discussion

In this paper, we have put some useful discussions related to the emergence of compact stars in the newly introduced $f(\mathcal{G}, T)$ theory of gravity by considering the model $f(\mathcal{G}, T) = \alpha\mathcal{G}^n + \lambda T$. We have tested this model for the strange star candidates Her X-1, SAX J 1808.4-3658, and 4U 1820-30 for anisotropic case by using the Krori and Barua approach of metric function [15], that is, $a = Br^2 + C$, $b = Ar^2$. The arbitrary constants A , B , and C are calculated by smoothly matching the interior metric conditions with the Schwarzschild's exterior metric conditions. This phenomenon makes us to understand the nature of the compact stars by expressing their masses and radii in terms of the arbitrary constants.

By using these constants in our investigation for the strange star candidates Her X-1, SAX J 1808.4-3658, and 4U 1820-30 the energy density, radial and tangential pressures have been plotted with respect to radial coordinate r indicating that when r approaches to zero, the density goes to its maximum for all the three strange star candidates. The same is the situation for the tangential pressure but different behavior in the case of the radial pressure for the 4U 1820-30 candidate. Mainly, this situation admits the theory that the core of compact stars under consideration, is intensely compact, particularly in case of the strange star candidate Her X-1. We have succeeded to determine the density of the emerging compact star ($\approx 1.5828 \times 10^{15} \text{ g cm}^{-3}$) after estimating the radius of the star ($R \approx 10$) from the evolution of the radial pressure. The evolution of EoS parameters with the increasing radius

satisfies the inequalities $0 < \omega_r < 1$ and $0 < \omega_t < 1$ for the radial and tangential EoS parameters respectively, which favor the acceptance of the model under study. We have also shown through the graphical representation that all the energy conditions namely NEC, WEC, SEC, and DEC are satisfied for the proposed $f(\mathcal{G}, T)$ gravity model in the case of Her X-1 favoring the physical viability of the model.

The static equilibrium, to some extent, has been established by plotting the three forces F_g , F_h , and F_a comprised in the TOV equation. The evolution of the radial and transversal sound speeds denoted by v_{sr}^2 and v_{st}^2 respectively for strange star candidate Her X-1 are within the bounds of stability [61], but in the case of SAX J 1808.4-3658, and 4U 1820-30 strange star candidates, the radial sound speed v_{sr}^2 evolutions temporarily violate these stability conditions. However, for the same candidates the transversal sound speeds v_{st}^2 are satisfied. Within the matter distribution, the estimation of the strongly stable and unstable eras from the differences of the propagations of the sound speeds satisfies the inequality $0 < |v_{st}^2 - v_{sr}^2| < 1$ for all the candidates as shown in Figure 11. Thus, overall the stability is attained for compact star $f(\mathcal{G}, T)$ model, particularly for the strange star candidate Her X-1.

We have also investigated the dynamical stability by analytically calculating the adiabatic index γ of the model both for the radial and tangential pressures for strange star candidate Her X-1, giving us $\gamma_r = 1.3757 > 4/3$ and $\gamma_t = 1.0597$, which shows the complete stability in radial case but a slight deviation in the tangential case. We have found the direct proportionality of the mass function to the radius, and $M(r) \rightarrow 0$ as $r \rightarrow 0$, suggesting that the mass function is regular at the center of the star. Moreover, for the spherically symmetric anisotropic fluid case, the ratio of the mass to the radius has been calculated as $\frac{2M}{r} = 0.4987$ satisfying $\frac{2M}{r} \leq \frac{8}{9}$ as proposed by Buchdahl [6]. The evolution of the compactness of the star for Her X-1 favors the model. The values of surface redshift function Z_S are within the bound of $Z_S \leq 2$ and for the case of the strange star candidate Her X-1, the redshift value is calculated as $Z_S \approx 0.22$ which satisfies the upper bound $Z_S \leq 2$. This further indicates the stability of the model under study. Conclusively, for the case of the strange star candidate Her X-1, all the physical parameters have been more consistent to favor the $f(\mathcal{G}, T)$ gravity model under study as compared to the other two candidates SAX J 1808.4-3658 and 4U 1820-30. The overall consistency for the model may be improved by considering some more suitable choices of the physical parameters.

Acknowledgement

Many thanks to the anonymous reviewer for valuable comments and suggestions to improve the paper. This work was supported by National University of Computer and Emerging Sciences (NUCES).

References

- [1] Sharif, M. and Ikram, A.: Eur. Phys. J. C **76** (2016) 640.
- [2] Oppenheimer, J.R. and Volkoff, G.: Phys. Rev. **55**(1939) 374.
- [3] Negele, J.W. and Vautherin D.: Nucl. Phys. A **207** (1973) 298.
- [4] Akmal, A., Pandharipande, V. R. and Ravenhall, D.G.: Phys. Rev. C **58** (1998) 1804.
- [5] Schwarzschild, K.: Sitzber. Preuss. Akad. Wiss. **189** (1916) 424.
- [6] Buchdahl, H. A.: Phys. Rev. **116** (1959) 1027.
- [7] Baade, W. and Zwicky, F.: Phys. Rev. **46** (1934) 76.
- [8] Longair, M.S.: *High Energy Astrophysics* (Cambridge University Press, 1994).
- [9] Ghosh, P.: *Rotation and Accretion Powered Pulsars*(World Scientific, 2007).
- [10] Ruderman, R.: Annu. Rev. Astron. Astrophys. **10** (1972) 427.
- [11] Maurya, S.K. and Gupta, Y.K.: Astrophys. Space Sci. **344** (2013) 243.
- [12] Maurya, S.K. and Gupta, Y.K.: Phys. Scr. **86** (2012) 025009.
- [13] Maharaj, S.D., Sunzu, J.M., and Ray, S.: Eur. Phys. J. Plus **129** (2014) 3.
- [14] Kalam, M. et al.: Eur. Phys. J.C **72** (2012) 2248.
- [15] Krori, K.D. and Barua, J.: J. Phys. A: Math. Gen. **8** (1975) 508.

- [16] Rahaman, F. et al.: Gen. Relativ. Grav. **44** (2012) 107.
- [17] Rahaman, F. et al.: Eur. Phys. J. C **72** (2012) 2071.
- [18] Mak, M.K. and Harko, T.: Int. J. Mod. Phys. D **13** (2004) 149.
- [19] Hossein, S.K.M. et al.: Int. J. Mod. Phys. D **21** (2012) 1250088.
- [20] Yazadjiev, S. S., Doneva, D. D. and Kokkotas, K. D.: Phys. Rev. D **91** (2015) 084018.
- [21] Staykov, K. V., Doneva, D. D., Yazadjiev, S. S. and Kokkotas, K. D.: JCAP **10** (2014) 006
- [22] Nojiri, S. and Odintsov, S.D.: Phys. Rep. **505** (2011) 59.
- [23] Paliathanasis, A et al.: Phys. Rev. D **89** (2014) 104042.
- [24] Nojiri, S. and Odintsov, S.D.: Int. J. Geom. Meth. Mod. Phys. **4** (2007) 115.
- [25] Capozziello, S., Laurentis, M. D. and Odintsov, S.D.: Eur. Phys. J. C **72** (2012) 2068.
- [26] Capozziello, S., Laurentis, M. D. Odintsov, S.D. and Stabile, A.: Phys. Rev. D **83** (2011) 064004.
- [27] Astashenok, A. V., Capozziello, S., Laurentis, M. D. and Odintsov, S.D.: JCAP **1501** (2015) 001.
- [28] Capozziello, S., Laurentis, M. D., Farinelli, R., and Odintsov, S.D.: Phys. Rev. D **93** (2016) 023501.
- [29] Felice, A.D. and Tsujikaswa, S.: Living Rev. Rel. **13** (2010) 3.
- [30] Bamba, K., Capozziella, S., Nojiri, S. and Odintsov, S.D.: Astrophys. Space Sci. **342** (2012) 155.
- [31] Astashenok, A.V., Capozziello, S. and Odintsov, S.D.: Phys. Rev. D **89** (2014) 103509.
- [32] Astashenok, A.V., Capozziello, S. and Odintsov, S.D.: JCAP **01** (2015) 001.

- [33] Cognola, G., Elizalde, E., Nojiri, S., Odintsov, S.D. and Zerbini, S.: Phys. Rev. D **73** (2006) 084007.
- [34] Shamir, M.F.: Astrophys. Space Sci. **361** (2016) 147.
- [35] Shamir, M.F.: J. Exp. Theor. Phys. **123** (2016) 607.
- [36] Nojiri, S. and Odintsov, S.D.: Phys. Lett. B **631** (2005) 1.
- [37] Chiba, T.: J. Cosmol. Astropart. Phys. **03** (2005) 008.
- [38] Nojiri, S. and Odintsov, S.D. and Tretyakov, P.V.: Prog. Theor. Phys. Suppl. **172** (2008) 81.
- [39] Starobinsky, A. A.: J. Exp. Theor. Phys. **86** (2009) 157.
- [40] Harko, T., Lobo, F.S.N., Nojiri, S. and Odintsov, S.D.: Phys. Rev. D **84** (2011) 024020.
- [41] Sharif, M. and Zubair, M.: J. Phys. Soc. Jpn. **82** (2013) 014002.
- [42] Sharif, M. and Zubair, M.: JCAP **03** (2012) 028.
- [43] Das, et al.: Astrophys. Space Sci. **358** (2015) 36.
- [44] Das, et al.: Eur. Phys. J. C **76** (2016) 654.
- [45] Sharif, M. and Yousuf, Z.: Astrophys. Space Sci. **354** (2014) 471.
- [46] Noureen, I. et al.: Eur. Phys. J. C **75** (2015) 323.
- [47] Zubair, M. and Noureen, I.: Eur. Phys. J. C **75** (2015) 265.
- [48] Zubair, M., Abbas, G. and Noureen, I.: Astrophys. Space Sci. **361** (2016) 8.
- [49] Shamir, M.F. and Ahmad, M.: Eur. Phys. J. C **77** (2017) 55.
- [50] Shamir, M.F. and Ahmad, M.: Mod. Phys. Lett. A **32** (2017) 1750086.
- [51] Cognola, G., Elizalde, E., Nojiri, S., Odintsov, S.D. and Zerbini, S.: Phys. Rev. D **75** (2007) 086002.
- [52] Cooney, A., DeDeo, S., and Psaltis, D.: Phys. Rev. D **82**(2010) 064033.

- [53] Ganguly, A., Gannouji, R., Goswami, R., and Ray, S.: Phys. Rev. D **89**(2014) 064019.
- [54] Momeni, D. and Myrzakulov, R.: Int. J. Geom. Methods Mod. Phys. **12** (2015) 1550014.
- [55] Astashenok, A. V., Capozziello, S., Laurentis, M. D. and Odintsov, S.D.: JCAP **1312** (2013) 040.
- [56] Lattimer, J.M. and Steiner, A.W.: Astrophys. J. **784** (2014) 123.
- [57] Li, X.D. et al.: Phys. Rev. Lett. **83** (1999) 3776.
- [58] Glendenning, N.K. *Compact Stars: Nuclear Physics, Particle Physics and General Relativity* (Springer, NewYork, 1997).
- [59] Herjog, M. and Roepke, F.K.: Phys. Rev. D **84** (2011) 083002.
- [60] Bhar, P., Rahaman, S., Ray, S. and Chatterjee, V.: Eur. Phys. J. C **75** (2015) 190.
- [61] Herrera, L.: Phys. Lett. A **165** (1992)) 206.
- [62] Chandrasekhar, S.: Astrophys. J. **140** (1964) 417.
- [63] Heintzmann, H. and Hillebrandt, W.: Astron. Astrophys. **38** (1975) 51.
- [64] Bondi, H.: Proc. R. Soc. Lond. Series A Math. Phys. Sci. **281** (1964) 39.